Appl Phys A (2010) 98: 249–254
DOI 10.1007/s00339-009-5389-6

Applied Physics A
Materials Science & Processing

Effect of Ta buffer layer and TaO_x barrier thickness on the evolution of the structural and magnetic properties of the $Fe/TaO_x/Co$ trilayers

H. Tokuc · S. Tari

Received: 2 March 2009 / Accepted: 10 August 2009 / Published online: 28 August 2009
© Springer-Verlag 2009

Abstract $Fe/TaO_x/Co$ trilayers were grown on Si(100)/SiO_2 substrates and on tantalum buffer layers by a high vacuum magnetron sputtering system. The effects of both Ta buffer layer and tantalum-oxide barrier layer thickness on the structural and magnetic properties and the coupling of the ferromagnetic layers have been studied. It was observed that Ta improves the structural properties of the Fe layer resulting in an increased coercive field. For a barrier thickness of 4 nm a weak decoupling starts to appear between the ferromagnetic layers and a clear step formation is observed with increasing thickness. The minor hysteresis loops predict an interlayer coupling for thin barriers. The annealing of trilayers up to 250°C shows an increased coercivity for only the Fe layer. Annealing further at 400°C has the opposite effect of decreasing the coercivity, indicating intermixing at the interfaces of the Fe. The refractive index of the insulator barrier shows that the barrier layer is not totally in the form of tantalum-pentoxide.

PACS 75.30.Gw · 75.60.Jk · 75.70.Ak · 75.70.Cn

1 Introduction

Magnetic tunnel junctions (MTJs) have a great potential for applications as magnetic recording heads and nonvolatile magnetic random access memories (MRAM) [1–3]. The growth of MTJs in general focused on using Al_2O_3 [4, 5] and MgO [6–8] extensively as insulator barrier layers. Barriers such as HfO_2 [9], $SrTiO_3$ [10], ZrO [11], $LaAlO_3$ [12] and TaO_x [13] have been reported in the literature. TaO_x, with the band gap of ~3.5 eV, results in a low barrier height of ~0.4 eV for ferromagnetic (FM)/TaO_x structures compared to other insulators. This allows for having relatively thicker barrier layers as well as a small resistance area (RA) product [14]. In addition, from the growth point of view, it is easier to grow thicker barriers with better uniformity and quality. The thicker barrier layers also decrease the orange peel coupling between the ferromagnetic layers. Moreover the interface morphology can affect the magnetic and transport properties of the MTJ. Magnetic properties such as coercivity, remanence and anisotropy of ferromagnetic materials are strongly influenced by their surface roughness [15], film thickness [16] and crystallinity [17]. TaO_x has been used as a barrier layer in the cobalt (Co) trilayers system [13] and a 1.5–2.5% magnetoresistance (MR) ratio was achieved at room temperature for thicknesses of 2.5–3 nm. Also, a 10% MR ratio was reported at room temperature by another group [18]. Therefore it is important to understand the properties of TaO_x as a barrier layer in MTJ structures.

In this study we report the growth of $Fe/TaO_x/Co$ trilayers, as a simple spin valve structure, on SiO_2 and on Ta layer using a Ta_2O_5 target. The effects of Ta and TaO_x barrier thickness, as well as annealing effect on the structural and magnetic properties of the trilayers have been studied.

2 Experimental details

All the layers were grown in a high vacuum (HV) chamber with the base pressure of about 1×10^{-7} Torr equipped with five magnetron guns, and a quartz crystal thickness monitor. The growth process is computer controlled; hence a

H. Tokuc · S. Tari (✉)
Department of Physics, Izmir Institute of Technology, Urla 35430
Izmir, Turkey
e-mail: suleymantari@iyte.edu.tr
Fax: +90-232-7507707

high degree of reproducibility is easily achievable. Fe, Ta and Co targets with 99.95% purity and Si(100)/SiO_2 (1 µm thermally grown) substrates were used. The substrate was rotated during the deposition to assure thickness uniformity. All the films were grown at ambient temperatures. Argon gas flow of 12 sccm assured 3 mTorr of deposition pressure. The targets were pre-sputtered in order to remove any contamination and oxidation of the surface prior to each layer deposition for 2 minutes. Various thicknesses of Ta, Fe and Co layers ranging from 4 to 70 nm were grown as a single layer and multilayers by DC sputtering. TaO_x barrier layers were grown by RF sputtering from a 2 inch Ta_2O_5 target with 99.9% purity. The growth rates were 0.2 Å/s for Fe and Ta, 0.1 Å/s for Co. Fe layers of 12 nm were used as the bottom and Co layers of 8 nm were used as the top FM electrode.

The structural properties of the films have been studied by X-ray diffraction (XRD) using the CuK_α line. The thicknesses of the layers were calibrated with a thickness monitor and compared with the thicknesses found from X-ray reflectivity (XRR) measurements. The thickness of TaO_x was measured with XRR as well as with ellipsometry. The surface roughness of the Ta layer was investigated with an atomic force microscope (AFM), and the magnetic hysteresis loops were recorded by a vibrating sample magnetometer (VSM), at room temperatures. Also the refractive index of the insulator barrier was measured by spectroscopic ellipsometry.

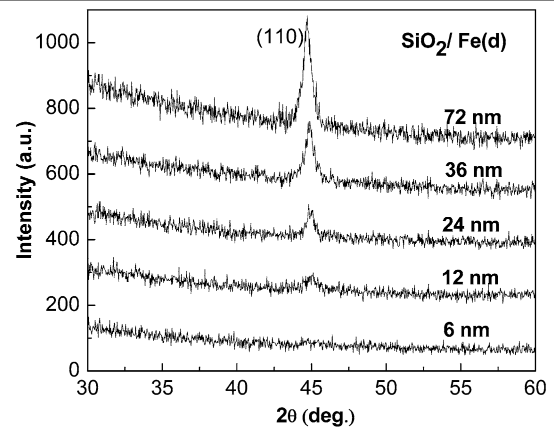

Fig. 1 The XRD patterns of various Fe layers grown on SiO_2

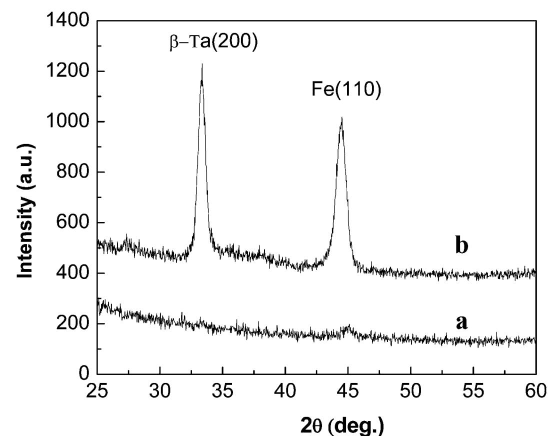

Fig. 2 The XRD patterns of (**a**) SiO_2/Fe(12 nm), (**b**) SiO_2/Ta(24 nm)/Fe(12 nm)

3 Results and discussion

The structure of single and multilayers were studied with XRD by θ–2θ scans. Figure 1 shows the XRD patterns of various thicknesses of Fe layers deposited on SiO_2. The peak at 44.96° for the 12 nm pattern belongs to the bcc Fe (110) planes. The FWHM of this Fe peak is 0.85 and the corresponding grain size calculated using the Scherer formula is 10.1 nm. As the thickness of the Fe film increases, the intensity of the peak increases. This increase is due to the fact that Fe continues growing in the preferred (110) orientation. The grain sizes also increase gradually and is found to be 16.1 nm for 72 nm of Fe. This indicates that the texture structure of the Fe layer is improving with thickness.

We also deposited Fe on SiO_2/Ta to study the effect of a Ta buffer layer on the structural and magnetic properties of the Fe layer. Figure 2 shows the patterns of 12 nm Fe grown on SiO_2 and on SiO_2/Ta (24 nm). As is seen clearly, the intensity of the Fe peak in the pattern (b) increases dramatically, compared to that of the Fe on SiO_2 for the same thickness shown in pattern (a). The Fe (110) peak is present at 44.42° with FWHM and grain size 0.72° and 11.9 nm, respectively. Although there is a large intensity increase, the grain size is not improving significantly compared to that of Fe on SiO_2 for the same thickness. Therefore we can associate the increase in the intensity with the better textured structure in the (110) direction of the Fe film. The peak at 33.31° belongs to the tetragonal-tantalum (β-Ta) (200) planes. A Ta film shows a strong texture in the (200) direction. It is well known that Ta has two structural phases, bcc cubic and β-Ta [19, 20]. The FWHM of this peak is 0.55° and the calculated grain size is 14.9 nm.

Co and Ta_2O_5 layers of thicknesses of 10 nm were grown on SiO_2. No diffraction peaks were observed for both layers. It is known that Ta_2O_5 shows a crystalline phase of the orthorhombic structure at about 500°C [21]. Although we do not see any signal in the XRD pattern for 10 nm of Co, it may be ordered (nanocrystals) to some extent. The fact that there is no observed diffraction peak may be due to the sensitivity of the X-ray detector. In fact, 10 nm of CoFe or even thinner has been shown to be crystalline [22]. Co layers show a texture phase at thicknesses above 40 nm, according to the XRD data. However, annealing of 25 nm Co at 450°C for one hour shows crystalline order. For this work we used

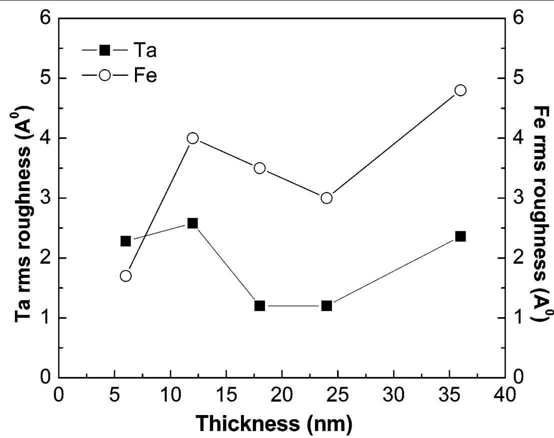

Fig. 3 Plot of rms roughnesses vs. thickness of Ta and Fe layers grown on SiO_2

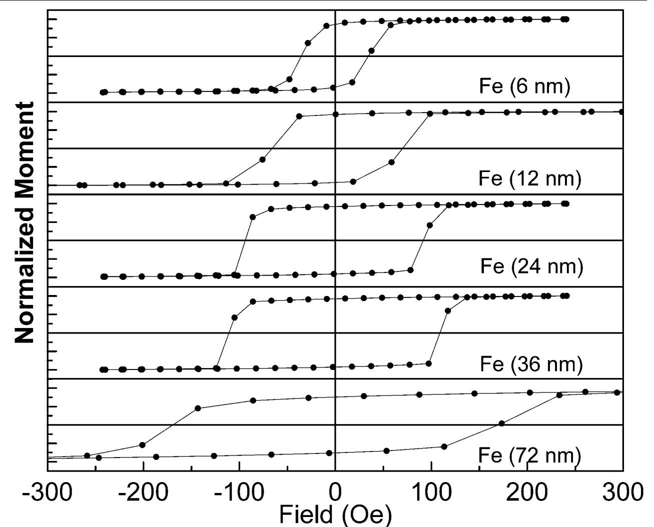

Fig. 4 Magnetic hysteresis loops of various thicknesses of Fe films grown on SiO_2. The magnetic field is applied in plane of the film in the [110] direction with respect to the Si substrate

8 nm of Co as the top FM electrode grown on the Ta_2O_5 barrier layer. Annealing the multilayer structure at 250°C does not affect the structure of the Co layer; however, it changes the structure of the Fe layer, affecting its magnetic properties. This is confirmed with magnetic measurements (see Fig. 9).

The surface of various thicknesses of thin Ta and Fe films grown on SiO_2 were studied by AFM with a scan area of 10 × 10 μm. Figure 3 shows the plot of the rms roughnesses of Ta and Fe layers vs. thickness. The rms roughness for Ta is between 1–3 Å and that of Fe is between 2–5 Å. The rms roughness of Fe(12 nm) grown on Ta(24 nm), which has the smoothest surface, was found to be 1.5 Å. This means that a Ta buffer layer not only improves the texture structure of the Fe layer but also results in smoother Fe surfaces. Roughnesses at the interfaces are crucial, which affects the roughness dependent magnetic coupling between the FM layers for thin barriers. The surface roughness also affects the magnetic properties to some extent.

Magnetic hysteresis loops (M-H) of single layers and multilayers were recorded by VSM. Figure 4 shows the M-H loops of various thicknesses of Fe layer grown on SiO_2 substrates. The applied magnetic field (H_{ex}) is in plane in the [110] direction with respect to the Si wafer. As the thickness of the Fe layer increases, the H_c increases. The increase in H_c is associated to the improvement of the texture of the thicker Fe layers as well as the roughness of the Fe surface, which increases slightly with the thickness causing pinning of the domain walls. For the Fe thickness of 6 and 36 nm, the H_c is 30 and 109 Oe, respectively. The shape of the hysteresis loops for all thicknesses is square-like. This indicates that the H_c of Fe is dominated by the domain wall motion [23]. The magnetization reversal for the Fe thickness of 76 nm is not falling sharply as seen in the other thicknesses. There may be contribution from a rotation of the domains to the H_c. H_{ex} was also applied in various angles in plane and no magnetic anisotropy has been detected for any thickness of the Fe layers. This also confirms that the H_c is dominated by the domain wall motion [24].

In order to investigate the effect of Ta buffer layer on the magnetic properties of a Fe film, 24 nm of Ta was deposited prior to Fe deposition. The H_c of Fe on the Ta film is almost three times larger than that of Fe on SiO_2, as is seen from the comparison of Figs. 5(a and c). This large change in H_c is mainly due to the improvement of the texture of the Fe layer deposited on Ta films as shown by the XRD pattern in Fig. 2. It is also possible that the Ta underlayer film might cause isolated grains within the Fe film by grain boundary segregation [25]. Therefore, the intrinsic H_c of these isolated grains causes the increase of H_c of Fe thin film, because domains do not interact with each other and rotate independently.

Metal Ta and insulator TaO_x layers were grown on SiO_2/Ta(24 nm)/Fe(12 nm) layer to determine the effect of oxidation on the magnetic properties of the Fe electrode independent of the completed trilayer structure. As seen in Figs. 5(c and d), capping the Fe layer with Ta increases the H_c from 185 to 224 Oe. The low H_c of Fe without Ta cap is associated to the oxidation of the top Fe layers after taking it to the atmosphere. The M-H loops of SiO_2/Ta/Fe/Ta, SiO_2/Ta/Fe/TaO_x are given in Figs. 5(d and e) for comparison. The H_c of SiO_2/Ta/Fe/Ta is 224 Oe and that of SiO_2/Ta/Fe/TaO_x is 165 Oe. The low H_c of the latter is again due to the oxidation at the interface of Fe/TaO_x; however, in this case the decrease in H_c is larger. The smallest coercivity of the Fe/TaO_x layer, ~53 Oe, (see Fig. 5b) with respect to the other layers also confirms the oxidation effect. We think that one of the reasons for these fluctuations in H_c is to some extent the oxidation of the top few layers of Fe films forming FeO_x, which is paramagnetic above 198 K

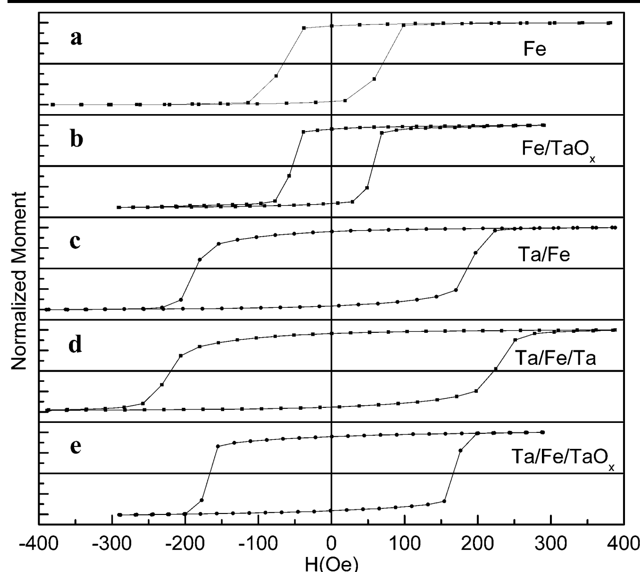

Fig. 5 Magnetic hysteresis loops of single layers and multilayers grown on SiO_2 substrates. In all loops Ta is 24 and Fe is 12 nm. (**a**) Fe, (**b**) Fe/TaO_x(8 nm), (**c**) Ta/Fe, (**d**) Ta/Fe/Ta and (**e**) Ta/Fe/TaO_x(8 nm)

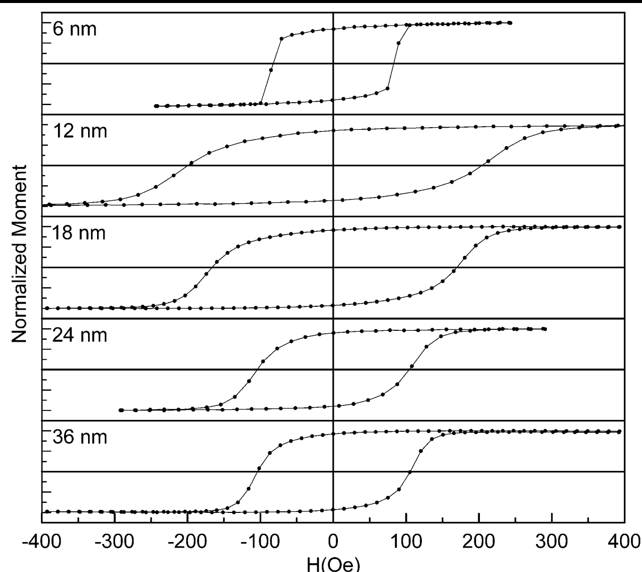

Fig. 6 Magnetic hysteresis loops of SiO_2/Ta(d)/Fe(12 nm)/TaO_x

[26]. Therefore the thickness of the ferromagnetic Fe layer decreases, resulting in a decrease in the H_c, because, as we see from Fig. 4, the H_c of the Fe films increases with the Fe thickness. These oxidized Fe layers might create dead magnetic layers, which diminishes the spin polarized transport of electrons.

We also investigated the effect of the Ta thickness on the magnetic properties of the Fe layer. Figure 6 shows the M-H loops of SiO_2/Ta(d)/Fe(12 nm)/TaO_x(4 nm) where d is the thickness. The H_c of Fe increases with increasing Ta thickness up to 12 nm and decreases afterwards. For thicknesses above 24 nm there is no significant change in H_c of Fe. We can associate this change in H_c to the structural changes of the Ta layer affecting the overlayer growth of the Fe film as its thickness increases. The trend in H_c change is possibly due to the stress build in the Fe film. It is well known that the structure of the ferromagnetic films strongly affects the magnetic properties [15–17]. The H_c is low for 6 nm Ta because at this thickness the Ta film might have not gained a crystalline order to induce a stress in the Fe film, whereas at 12 nm of Ta, which is likely to have a better crystalline order, it creates more stress in the Fe film due to the large lattice mismatch and hence the largest H_c is observed. After some critical thickness in thin films the stress is relaxed by the introduction of defects. The H_c is decreasing and staying almost the same for further thicknesses of Ta indicating that the Ta film is stress free; hence the structure of Fe grown after about 24 nm does not change significantly. It is also possible that the surface roughness of the Ta film, which changes to some extent, might contribute to the magnetic properties of the Fe film.

After determining the H_c of the bottom Fe contact layers the multilayer stack using Co as the top electrode was grown. From the magnetic characterization of the Co films of various thicknesses grown on Si we observed that the H_c of Co decreases from 75 to 25 Oe for 4 and 15 nm, respectively, and increases gradually after 25 nm of thickness. The H_c and M_s of ferromagnetic films depend strongly on the film thickness [27]. The initial decrease in H_c of the thin Co layer may be associated with the formation of CoO on top of the Co film, because the magnetic effects of antioferromagnetic layers are inversely proportional with the magnetic film thickness. The presence of the CoO on top of the Co films has no effect for thick layers. The effect of CoO on the properties of the Co thin film has been studied in the literature [28]. Another possible explanation is the presence of stress in thin Co layers. Above 40 nm of thickness, where Co has textured structure according to XRD, H_c starts increasing linearly because of an increase in grain size. Large grains cause a large H_c [29]. A similar behavior is also seen for Co films grown by the evaporation technique [30]. The thickness of the TaO_x is changed to see the evolution of the decoupling between the top and bottom FM electrodes. Figure 7 shows the M-H loops of the SiO_2/Ta(24 nm)/Fe(12 nm)/TaO_x(d)/Co(8 nm) structure, where d is the thickness. There is a strong coupling between Fe and Co layers for the 4 nm of TaO_x barrier. Actually for this thickness a decoupling would be expected. One of the reasons for this coupling might be the possibility that TaO_x is not yet a uniform continuous film. A second reason may be the roughness of TaO_x interfaces, which may cause orange peel coupling. It is also possible that there is an indirect exchange coupling through the TaO_x layer, since according to the ellipsometry data the barrier layer is not to-

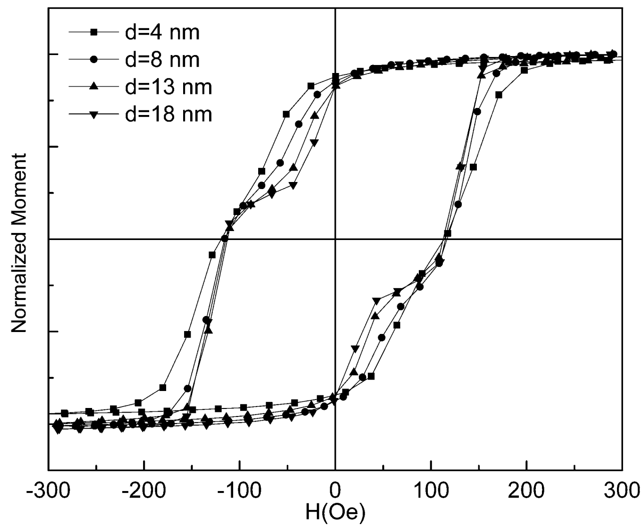

Fig. 7 Magnetic hysteresis loops of SiO_2/Ta(24 nm)/Fe(12 nm)/$TaO_x(d)$/Co(8 nm) MTJ where d is the thickness of the TaO_x barrier layer

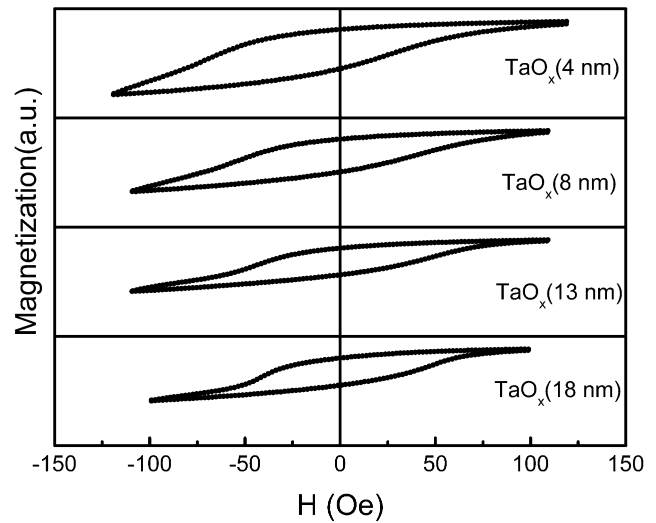

Fig. 8 M-H minor loops of Co layer in the Ta(24 nm)/Fe(12 nm)/$TaO_x(d)$/Co(10 nm) structure

tally in the form of Ta_2O_5 and suboxides exists. At this point we cannot say much about the phase of the barrier layer and which mechanism for the coupling is likely. For 8 nm TaO_x barrier thickness there is a kink at the loop indicating that the coupling is getting weaker. As the thickness of the TaO_x increases, a clear step representing two different coercivity values is observed with H_c of Co ~50 Oe and H_c of the Fe layer ~130 Oe. For the 18 nm TaO_x there is a total decoupling between the FM layers.

To identify the coupling mechanism and strength of the coupling field, minor loops of the Co layers were measured for each MTJ stack, while the magnetization of the hard layer remains in the remanent state. Figure 8 shows the corresponding minor loops of the Co layer. There is a strong shift in the minor loop of TaO_x (4 nm), which may be an indication of a magnetostatic Néel coupling field [31] ($H_N = 24$ Oe) due to the correlated interface roughness of the two ferromagnetic electrodes at the barrier interfaces. However, at this point we cannot be certain about the mechanism of coupling. Further work, especially transmission electron microscopy (TEM) cross section revealing the roughness of the interfaces, could help to determine the dominant coupling mechanism. The further increase of the barrier thickcess causes a reduction in the H_N with values of 16, 8 and 5 Oe for 8, 13 and 18 nm, respectively. A larger coupling field is expected for a small barrier because the Néel coupling field increases exponentially with decreasing barrier thickness. For small barrier thicknesses, it is hard to determine the contribution of each layer to the total magnetization because not all of the Co moments had reversed before the moments of Fe switched. The H_c of Co was about 44 Oe (at the inflection point) for a MTJ stack layer with TaO_x (4 nm) and it decreases to the 41, 38 and 35 Oe for barrier thicknesses of 8, 13 and 18 nm, respectively, and also a sharper switching behavior is observed with increasing thickness. Another reason for a larger H_c for a small spacer might be coming from the lock-in of stray fields, generated by domain walls and a magnetization ripple in the Co layer, by the hard layer stray fields associated with domain walls and magnetization ripples in the hard layer [32].

In order to study the effect of the annealing on the coupling mechanism the SiO_2/Ta(24)/Fe(12)/$TaO_x(d)$/Co(8) multilayers were annealed at different temperatures. The M-H loops of annealed multilayers with 18 nm TaO_x barrier thickness along with as-deposited ones is shown in Fig. 9. This sample was annealed at 100, 250 and 400°C. H_c of the as-deposited Fe layer is 125 Oe and it increases with an increasing annealing temperature and reaches 225 Oe for 250°C. There is a slight change in the H_c of the top Co layer. The increase in H_c of the Fe layer results from the improvement of the structure of the Fe layer with annealing. Also the roughness of the Fe/TaO_x interface is likely to decrease with annealing resulting in a decrease in magnetostatic coupling. This decrease in coupling may be due to the oxygen redistribution and homogenization in the TaO_x barrier during the annealing process [33]. However, the H_c of the Fe layer annealed at 400°C decreases to 150 Oe. This decrease in H_c is believed to result from intermixing at the Fe/TaO_x interfaces by interdiffusion of Fe, oxygen or Ta. It is known that at about 200°C Fe starts diffusing. Similar behaviors have been observed from M-H loops of the MTJ with barrier layer thicknesses of 4, 8, and 13 nm grown and annealed at the same conditions as well.

The stoichiometry of the TaO_x films grown on Si was measured by ellipsometry. The refractive index (n) for Ta_2O_5 is 2.2; however, the n for our films sputtered from a Ta_2O_5 target was found to be 2.59, indicating that our in-

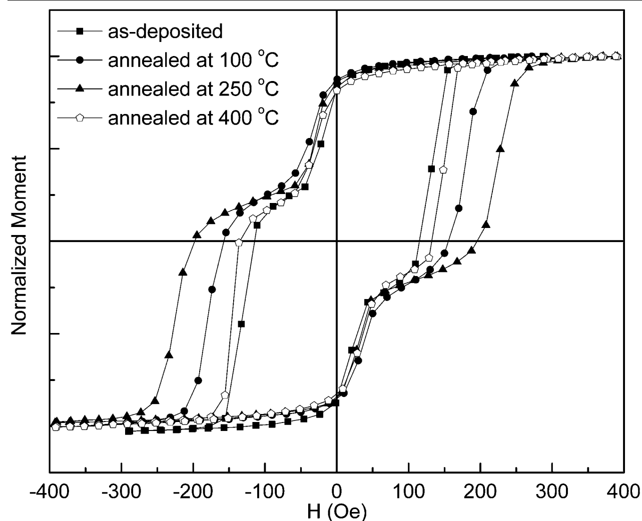

Fig. 9 Magnetic hysteresis loops of annealed SiO_2/Ta(24 nm)/Fe(12 nm)/TaO_x(18 nm)/Co(8 nm) at different temperatures

sulator layers are likely to have suboxides in the form of Ta-oxide [34].

4 Conclusions

Ta buffer layer improves the structure of the Fe layer significantly. The H_c of the Fe layers on Ta were found to be almost three times larger than that of Fe on SiO_2. The TaO_x barrier layer thickness dependence of the Ta/Fe/TaO_x/Co structure indicates that the coupling may be due to magnetostatic coupling. M-H minor loops, especially for thin layers of TaO_x, support this result to some extent. However, for 4 nm of TaO_x indirect exchange coupling might also contribute to the coupling mechanism. Annealing of the multilayers up to 250°C resulted in an increase of the H_c of the bottom Fe layer. Sputtered insulator thin films from a Ta_2O_5 target result in suboxide formation indicating lack of oxygen. Hence suboxides in the form of Ta_xO_y along with stoichiometric Ta_2O_5 might exist.

Acknowledgements This work is supported by The Scientific & Technological Research Council of Turkey under Grant No. TBAG-105T109. We thank Dr. S. Okur for AFM and Dr. G. Aygun for ellipsometry measurements.

References

1. G.A. Prinz, Science **282**, 1660 (1998)
2. I. Zutic, J. Fabian, D. Sarma, Rev. Mod. Phys. **76**, 323 (2004)
3. S. Ikeda, J. Hayakawa, Y. Min Lee, F. Matsukara, Y. Ohno, IEEE Trans. Electron. Dev. **54**(5), 991 (2007)
4. J.S. Modera, L.R. Kinder, T.M. Wong, R. Meservey, Phys. Rev. Lett. **74**, 3273 (1995)
5. M. Mizuguchi, Y.M. Suzuki, T. Nagahama, S. Yuasa, Appl. Phys. Lett. **87**, 171909 (2005)
6. S. Yuasa, T. Katayama, T. Nagahama, A. Fukushima, H. Kutaba, Appl. Phys. Lett. **87**, 222508 (2005)
7. S. Yuasa, T. Nagahama, A. Fukushima, Y. Suzuki, K. Ando, Nat. Mater. **3**, 868 (2004)
8. Y.M. Lee, J. Hayakawa, S. Ikeda, F. Matsukara, H. Ohno, Appl. Phys. Lett. **90**, 212507 (2007)
9. C.L. Flatt, B. Dieny, A.E. Berkowitz, J. Appl. Phys. **81**, 5523 (1997)
10. J.M. De Teresa, A. Barthelemy, A. Fert, J.P. Contour, R. Lyonnet, F. Montaigne, P. Seneor, A. Vaures, Phys. Rev. Lett. **82**, 4288 (1999)
11. J. Wang, P.P. Freitas, E. Snoeck, P. Wei, J.C. Soares, Appl. Phys. Lett. **79**, 4387 (2001)
12. V. Garcia, M. Bibes, J.L. Maurice, E. Jacquet, K. Bouzehouane, J.P. Contour, A. Barthelemy, Appl. Phys. Lett. **87**, 212501 (2005)
13. P. Rottlander, M. Hehn, O. Lenoble, A. Schuhl, Appl. Phys. Lett. **78**, 3274 (2001)
14. L.S. Dorneles, R.L. Sommer, L.F. Schelp, J. Appl. Phys. **91**, 7971 (2002)
15. M. Li, G.-C. Wang, J. Appl. Phys. **83**, 5313 (1998)
16. A. Kharmouche, S.-M. Chérif, A. Bourzami, Layadi, G. Schmermer, J. Phys. D, Appl. Phys. **37**, 2583 (2004)
17. A. Sharma, R. Brajpuria, S. Tripathi, S.M. Chaudhari, J. Vas. Sci. Technol. A **24**(1), 74 (2006)
18. M.F. Gillies, A.E.T. Kuiper, J.B.A. Van Zon, J.M. Sturn, Appl. Phys. Lett. **78**, 3498 (2001)
19. A. Jiang, T.A. Tyson, L. Axe, L. Gladczuk, M. Sosnowski, P. Cote, Thin Solid Films **479**, 166 (2005)
20. L. Liu, Y. Wang, H. Gong, J. Appl. Phys. **90**, 416 (2001)
21. H.S. Cheng, C.T. Mao, Mater. Res. Bull. **38**, 1841 (2002)
22. J. Joshua Young, A.K. Bengtson, C.X. Ji, D. Morgan, A. Chang, J. Appl. Phys. **103**, 056102 (2008)
23. J. Swerts, S. Vandezande, K. Temst, C. Van Haesendonck, Solid State Commun. **131**, 359 (2004)
24. M. Li, Y.P. Zhao, G.C. Wang, H.G. Min, J. Appl. Phys. **83**, 6287 (1998)
25. R.L. Comstock, *Introduction to Magnetism and Magnetic Recording* (Wiley, New York, 1999), p. 424
26. C. Park, J.G. Zhu, Y. Peng, D.E. Laughlin, R.M. White, J. Appl. Phys. **97**, 10C907 (2005)
27. M.L. Munford, L. Seligman, M.L. Sartorelli, E. Voltolini, L.F.O. Martins, W. Schwarzacher, A.A. Pasa, J. Magn. Magn. Mater. **226**, 1613 (2001)
28. T.R. McGuire, T.S. Plaskett, R.J. Gambio, IEEE Trans. Magn. **29**(6), 2714 (1993)
29. J. Islam, Y. Yamamoto, H. Hori, J. Magn. Magn. Mater. **310**, 2234 (2007)
30. A. Sharma, S. Tripathi, R. Brajpuria, T. Shripathi, S.M. Chaudhari, J. Nanosci. Nanotechnol. **7**, 2041 (2007)
31. L. Néel, Ann. Phys. (N.Y.) **2**, 61 (1967)
32. H.D. Chopra, D.X. Yang, P.J. Chen, D.C. Parks, W.F. Egelhoff Jr., Phys. Rev. B **61**, 9642 (2000)
33. K.I. Lee, J.H. Lee, W.Y. Lee, K.W. Rhie, J.G. Ha, C.S. Kim, K.H. Shin, J. Magn. Magn. Mater. **239**, 120 (2002)
34. J.Y. Zhang, I.W. Boyd, Appl. Phys. A **70**, 657 (2000)